

Development of Biocompatible Mussel-Inspired Cellulose-Based Underwater Adhesives

Zuwu Tang, Xinxing Lin,* Meiqiong Yu, Ajoy Kanti Mondal,* and Hui Wu*

Cite This: *ACS Omega* 2024, 9, 3877–3884

Read Online

ACCESS |



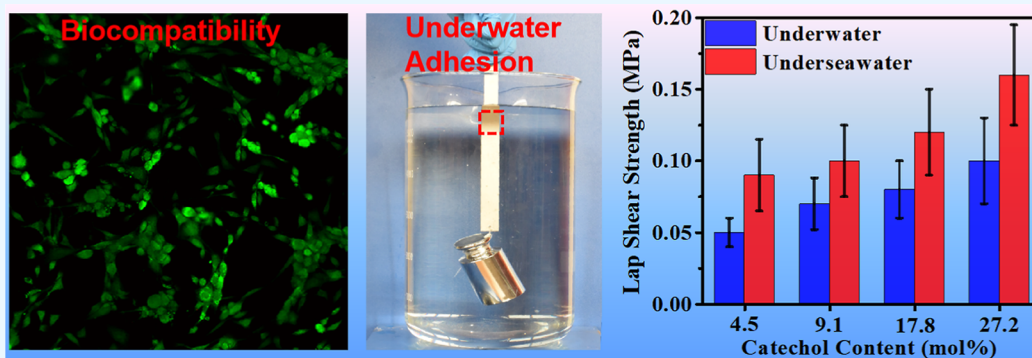
Metrics & More



Article Recommendations



Supporting Information



ABSTRACT: Conventional adhesives have poor underwater adhesion and harm to human health and the environment during their use, which largely limits their practical applications. Herein, we synthesized cellulose-based adhesives with underwater adhesion and biocompatibility by grafting *N*-(3,4-dihydroxyphenethyl)methacrylamide into the cellulose chain via atom transfer radical polymerization (ATRP). FTIR, ^1H NMR, and XPS analyses ensured the successful preparation of the cellulose-based adhesive polymers. The different properties of the prepared adhesives, including swelling ratio, adhesion strength, and biocompatibility are examined. Results found that the lap shear strength is enhanced by increasing the catechol content. When catechol content is 27.2 mol %, cellulose-based adhesive with the addition of Fe^{3+} possesses a strong lap shear strength of 2.13 MPa in a dry environment, 0.10 MPa underwater, and 0.16 MPa under seawater for iron substrate, respectively. In addition, the cell culture test demonstrated that the prepared adhesives have outstanding biocompatibility. The cellulose-based adhesives with underwater adhesion and biocompatibility have potential applications in biomedicine, electronic engineering, and construction fields.

1. INTRODUCTION

Strong adhesion is a major topic in adhesion science and technology.^{1,2} However, it is difficult to meet this requirement in a wet environment or underwater because water molecule can act as a plasticizer, which can weaken the interfacial adhesion of the adhesive and destroy its integrity.^{3,4} Although some underwater adhesives have been developed, most polymeric adhesives are made of petroleum-based polyurethane, epoxy, and cyanoacrylate,^{5–7} leading to a certain degree of biological toxicity or being environmentally unfriendly.^{8,9} Thus, one of the big challenges in the field of adhesion science and technology is to formulate smart materials with underwater adhesion capability and biocompatibility.

In nature, different marine organisms, including mussels,^{10–12} sandcastle worms,^{13–15} and barnacles,^{16,17} direct a strong wet adhesion mechanism via the elegant combination of catechol chemistry, polyelectrolyte complexes, and supramolecular architectures.^{18–20} This is due to the excellent wet adhesion tenacity that can be mimicked or competed with by the use of 3, 4-dihydroxy-L-phenylalanine (DOPA) groups.^{21,22}

The catechol acts as a crucial functional group on various substrates through catechol chemistry,²³ including hydrogen bonding, π - π interactions, metal coordination, Schiff base reaction or Michael addition, cation- π interactions, hydrophobic interactions, boronate-catechol complexation, and covalent bonds. Based on their understanding of adhesion mechanisms, researchers have also gradually developed a variety of adhesive materials for potential applications, such as bioelectronics²³ and biomedicines.^{24–28}

Cellulose is one of the most abundant polysaccharides, with high availability, biodegradability, biocompatibility, and good mechanical properties.²⁹ The hydroxyl groups on anhydroglucose units fit cellulose to be appropriate for a diversity of

Received: October 11, 2023

Revised: December 23, 2023

Accepted: December 28, 2023

Published: January 6, 2024



physical or chemical modifications. Especially, various monomers are grafted onto the cellulose backbone by atom transfer radical polymerization (ATRP), which is expected to produce functional materials. They could combine the advantages of synthetic polymer and natural polymer properties, which have been widely used in various fields such as biomedicines,^{30,31} bioelectronics,^{32,33} energy,^{34–37} and environment.^{38–40}

Inspired by this, the aim of this research is to design mussel-inspired cellulose-based adhesives with strong underwater adhesion and biocompatibility. The cellulose-based adhesive was obtained by grafting catechol groups onto cellulose via ATRP. The mechanical properties of the prepared adhesives on different substrates were assessed under both dry and wet conditions. The adhesives exhibited excellent biocompatibility. Depending on their excellent underwater adhesion and biocompatibility, this study presents great potential for cellulose-based adhesives for different applications in biomedicine, electronics, and wood processing.

2. MATERIALS AND METHODS

2.1. Materials. The wood-dissolving pulp was received from Qingshan Paper Co., Ltd., Fujian, China. 2-Bromoisobutyl bromide, cuprous bromide (CuBr), *N,N*-methylacetamide (DMAc), dichloromethane (CH₂Cl₂), pyridine, lithium chloride (LiCl), ethanol, dimethyl sulfoxide (DMSO), 3,4-dihydroxyphenylalanine hydrochloride (DOPA-HCl), triethylamine (TEA), triethylchlorosilane, methacryloyl chloride, *n*-hexane, sodium sulfate (Na₂SO₄), ethyl acetate, *N,N*-dimethylformamide (DMF), and *N,N,N',N',N''*-pentamethyldiethylenetriamine (PMDETA), were bought from Sinopharm Group Chemical Reagent Co., Ltd., Tianjin, China.

2.2. Preparation of Cellulose-Based Adhesives. The protected dopamine methacrylamide (protected DOPMAM) and cellulose-based macroinitiator were prepared according to the published literature.⁴¹ For the protected DOPMAM, DOPA-HCl, TEA, triethylchlorosilane, and methacryloyl chloride were added to a three-neck flask with CH₂Cl₂. The above mixture was stirred continuously at room temperature. After the reaction, the protected DOPMAM was obtained by evaporating, extracting with ethyl acetate, washing with brine, drying with Na₂SO₄, and purifying with an *n*-hexane/ethyl acetate mixture. For the cellulose-based macroinitiator, cellulose was dissolved in a DMAc/LiCl solution. Then, pyridine and 2-bromoisobutyl bromide were added and stirred. Finally, the cellulose-based macroinitiator was obtained through precipitating and drying.

0.311 g (1 mmol of anhydroglucose units) of cellulose-based macroinitiator, protected DOPMAM with different catechol contents, 144 mg (1 mmol) of CuBr, and 0.63 mL (3 mmol) of PMDETA were mixed to 20 mL of DMF, as shown in Table 1. The oxygen in the flask was removed, and the

copolymerization was accomplished at 60 °C for 14 h. After that, the deprotection was carried out using 1 mol L⁻¹ HCl (Figure 1). Finally, the cellulose-based adhesives were obtained by purifying and drying, and the pH of the adhesives was about 6.8.

2.3. Characterization. The adhesives were characterized by Fourier-transform infrared spectroscopy (FTIR, BRUKER TENSOR II, Germany), proton nuclear magnetic resonance (¹H NMR, BRUKER AVANCE III 500, Switzerland) spectroscopy, and X-ray photoelectron spectroscopy (XPS, Thermo Scientific ESCALAB 250Xi, USA). FTIR spectra were recorded using the frequency range from 4000 to 400 cm⁻¹. ¹H NMR spectroscopy was accomplished on an S4300 MHz Bruker NMR instrument with MestReC processing software. XPS was used to confirm the structure of the samples.

2.4. Swelling Ratio. The swelling behavior of the adhesives was tested at room temperature. The weight of the dry adhesives was measured (*m*₀) and then swallowed in 50 mL of pure water. After that, the weight of the immersed samples was measured (*m*_t) with maintenance of the time intervals. The swelling ratio (SR) was determined by following eq 1⁴¹

$$SR = \frac{m_t - m_0}{m_0} \times 100\% \quad (1)$$

2.5. Biocompatibility. The biocompatibility of the adhesives was evaluated. NIH-3T3 cells were cultured in Dulbecco's minimum essential medium (DMEM) bearing 10% fetal bovine serum (FBS) and 1% antibiotics. First, the adhesives were cut in a cuboid (2 mm × 1 mm × 1 mm), which were washed with PBS and UV-sterilized for 30 min. Second, the cells on the adhesives were cultured into 96-well plates with a concentration of 10⁵ cells/well. Third, the cells were cultured for 1 and 5 days. Fourth, the growth of the cells was measured by the MTT assay, and the relative cell viability was calculated by following eq 2²⁴

$$\text{Relative cell viability} = \frac{A_{\text{adhesive}}}{A_{\text{control}}} \times 100\% \quad (2)$$

where *A*_{adhesive} and *A*_{control} are the absorbances of cells cultured in the adhesive and in the cell culture medium, respectively.

2.6. Lap Shear Strength. The lap shear strength was measured with different substrates, including glass, wood, iron, and Al, which were washed with ultrapure water and methanol subsequently and dried at 50 °C before use.⁴² For adhesion experiments, 0.30 g of adhesives with Fe³⁺ content to catechol was dissolved in 1.0 mL of DMSO. 45 μL portion of the adhesive solution was coated on the adherents and then overlapped (1.5 × 1.0 cm) at room temperature. The adhesive sample was left for 48 h in an open space to evaluate the adhesion properties in the dry state. Before the measurement of water resistance, the adherent was submerged in water for 24 h at room temperature. Then, the sample was taken, and the lap shear strength was calculated by following eq 3⁴³

$$\tau = \frac{F}{S} \quad (3)$$

where τ , *F*, and *S* represent the lap shear strength (Pa), the maximum load (N), and the area of the overlapped adherents (m²), respectively.

Table 1. Catechol Content in Adhesive with Different Ratios of DOPMAM

feeding ratio (<i>n</i> _{DOPMAM} / <i>n</i> _{cell})	catechol content (mol %)
5:95	4.6
10:90	9.1
20:80	17.8
30:70	27.2
40:60	27.2

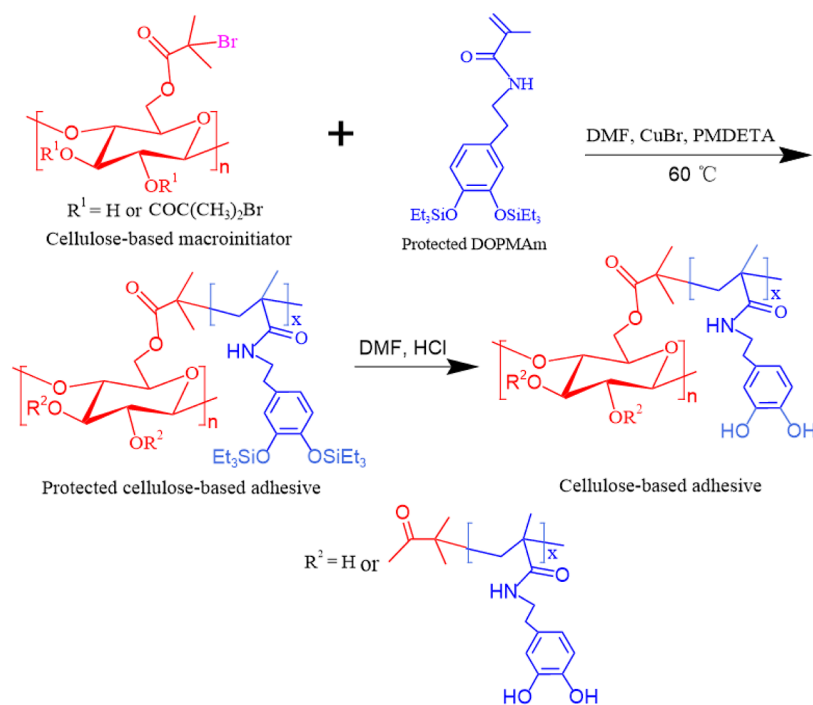


Figure 1. Synthesis of cellulose-based adhesives.

3. RESULTS AND DISCUSSION

3.1. Preparation and Characterization of Cellulose-Based Adhesives. The cellulose-based adhesives were

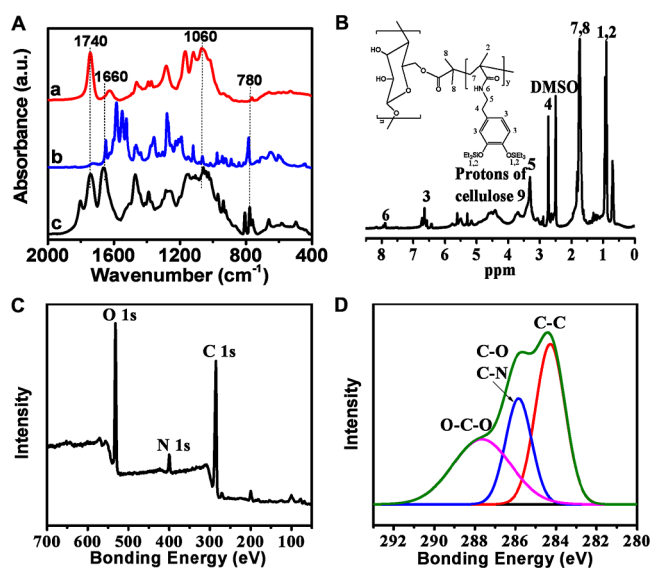


Figure 2. (A) FTIR spectra of (a) cellulose-based macroinitiator, (b) DOPMam, and (c) cellulose-based adhesive. (B) ^1H NMR spectra, (C) XPS spectra of the survey scan, and (D) XPS spectra of C 1s scan of cellulose-based adhesive.

prepared via the following steps. First, the protected DOPMam was synthesized using DOPA·HCl, triethylchlorosilane, and methacryl chloride. Second, the cellulose-based macroinitiator was synthesized using 2-bromoisobutyryl bromide. Third, the protected cellulose-based adhesives were synthesized by grafting protected DOPMam onto a cellulose-based macroinitiator via ATRP. Fourth, the protected cellulose-based adhesives were deprotected by HCl solution

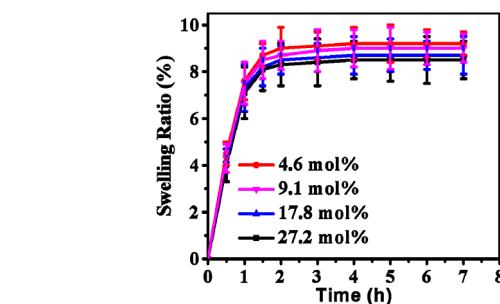


Figure 3. SR of cellulose-based adhesives.

(Figure 1). To explore the effect of the amount of catechol on the lap shear strength, a number of cellulose-based adhesives with different catechol contents ranging from 4.6 to 27.2 mol % were prepared (Table 1).

The structure of the cellulose-based macroinitiator, DOPMam, and cellulose-based adhesive was characterized by using FTIR, as shown in Figure 2. The vibrational band of C–O on the cellulose backbone is located at 1060 cm^{-1} (Figure 2a–c). A strong absorption peak at 1740 cm^{-1} represents the C=O stretching vibration (Figure 2a–c). A sharp peak at 1660 cm^{-1} is attributed to the amide I band (Figure 2b,c). The methylene peak associated with the benzene ring is located at 780 cm^{-1} (Figure 2b,c). All of these results suggest that the cellulose-based macroinitiator, DOPMam, and cellulose-based adhesive were successfully synthesized.

Figure S1 shows the ^1H NMR spectra of DOPMam and the cellulose-based macroinitiator. The proton peaks of ethyl groups (peak h) are observed at 0.5–1.0 ppm (Supporting Information, Figure S1AI). The proton peaks of catechol groups in the benzene ring are situated at 6.7 ppm (peak g). The methylene group peaks are at 3.5 ppm (peak e) and 2.7 ppm (peak f), respectively. The methyl group peak is at 1.9 ppm (peak c). The methylene group peaks on the double bond

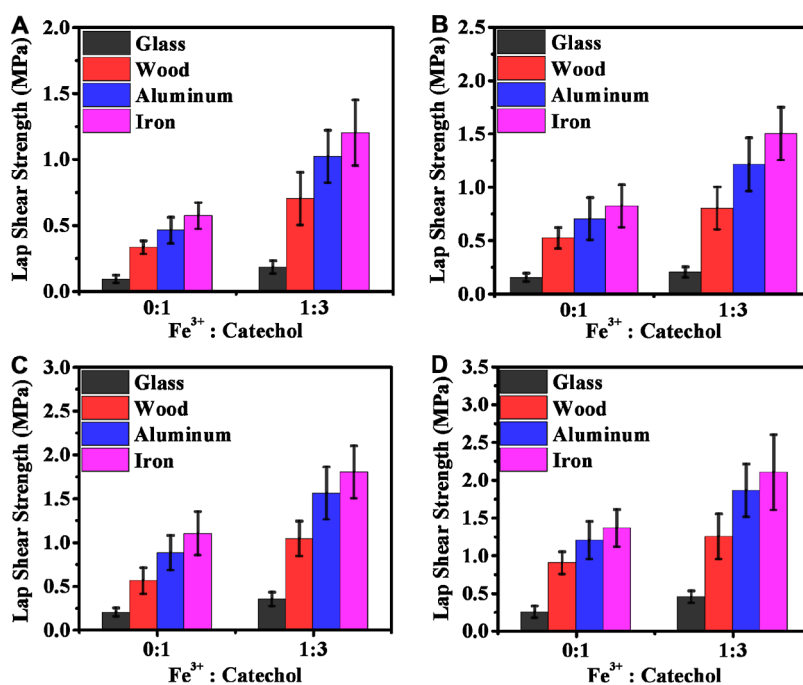


Figure 4. Lap shear strength of the cellulose-based adhesives: (A) 4.6 mol %, (B) 9.1 mol %, (C) 17.8 mol %, and (D) 27.2 mol %.

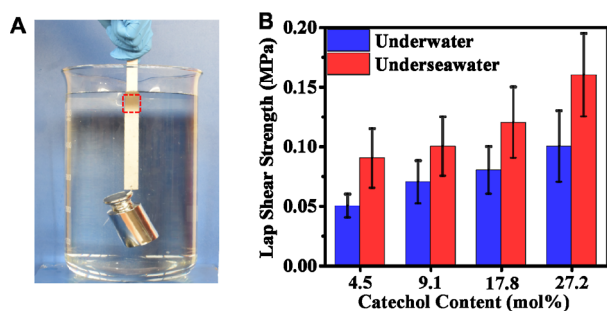


Figure 5. (A) Underwater iron adherents lifted 500 g weight applying the prepared adhesive. (B) Lap shear strength of adhesives with Fe^{3+} on iron substrates in a wet environment.

are at 5.3 and 5.6 ppm (peaks a, b). To distinguish the catechol groups in the protected and unprotected DOPMAM, the proton peaks of ethyl groups in the protected groups for the protected DOPMAM could not be observed for the unprotected DOPMAM (Supporting Information, Figure S1AII). Figure S2B shows the ^1H NMR spectra of a cellulose-based macroinitiator. The proton peaks of methyl (peak a) are located at 1.7 ppm. The proton peaks of cellulose are observed at 3.0 and 3.5–4.8 ppm. These results indicate that DOPMAM and cellulose-based macroinitiators were successfully synthesized.

To further confirm that the cellulose-based adhesive was successfully synthesized, the ^1H NMR spectrum was characterized. As shown in Figure 2B, the proton peaks of DOPMAM (peak 1,2) are observed at 0.5–1.0 ppm.²¹ The proton peaks of catechol groups in the benzene ring are situated at 6.7 ppm (peak 3). Figure 2B represents the methylene group peaks of DOPMAM at 3.2 ppm (peak 5) and 2.7 ppm (peak 4), respectively. Similarly, the amide bond is confirmed by the proton peak (peak 6) at 7.9 ppm. Methyl peaks on cellulose were at 1.5–2.0 ppm. The proton peak of

cellulose (peak 9) was located at 3.5–5.8 ppm. These results indicate that DOPMAM was grafted onto cellulose.

To further confirm that the cellulose-based adhesive was successfully synthesized, XPS was used to characterize. As shown in Figure 2C,D, the XPS spectrum depicted O 1s, N 1s, and C 1s peaks at 533.1, 400.1, and 285.1 eV, respectively (Figure 2C). In the C 1s spectra (Figure 2D), the peaks of the adhesive at positions 288.5, 286.4, and 284.8 eV are mainly assigned to the bonds of O–C–O, C–O/C–N, and C–C, respectively. These results also indicate that DOPMAM was grafted onto cellulose.

3.2. Swelling Ratio. The SR of the adhesive is a significant influence for underwater adhesion. When the adhesives are immersed in water, they may spread into the inner of the adhesive or the interfaces among the adhesive and substrates, developing volume expansion and leading to the collapse of the adhesion. In this case, measurement of the SR is an important parameter of adhesives. The SR of adhesives is shown in Figure 3. Results demonstrate that, when the catechol content of the adhesive is 4.6 mol %, its SR in the first 2 h is 9.5%. Then, with an increase in time, no significant change is observed in the SR. With increasing the amount of catechol from 4.6 to 27.2 mol %, the SR of adhesives decreased insignificantly from 9.5 to 8.5% gradually. These results indicate that the cellulose-based adhesives are hard to affect by water.

3.3. Lap Shear Strength. Figure 4 shows the lap shear strength of the cellulose-based adhesives on various substrates. When the catechol content is 4.6 mol %, the weakest lap shear strength is shown on various substrates, which has only 0.09 MPa on glass, 0.33 MPa on wood, 0.46 MPa on aluminum, and 0.57 MPa on iron (Figure 4A). With the increase of catechol content, the lap shear strength becomes stronger gradually. The strongest lap shear strength is increased to 0.25 MPa on glass, 0.90 MPa on wood, 1.20 MPa on aluminum, and 1.47 MPa on iron when the catechol content is 27.2 mol % (Figure 4D). To improve the lap shear strength, 1 mole of Fe^{3+} with 3 moles of catechol is coordinated, which can form stable

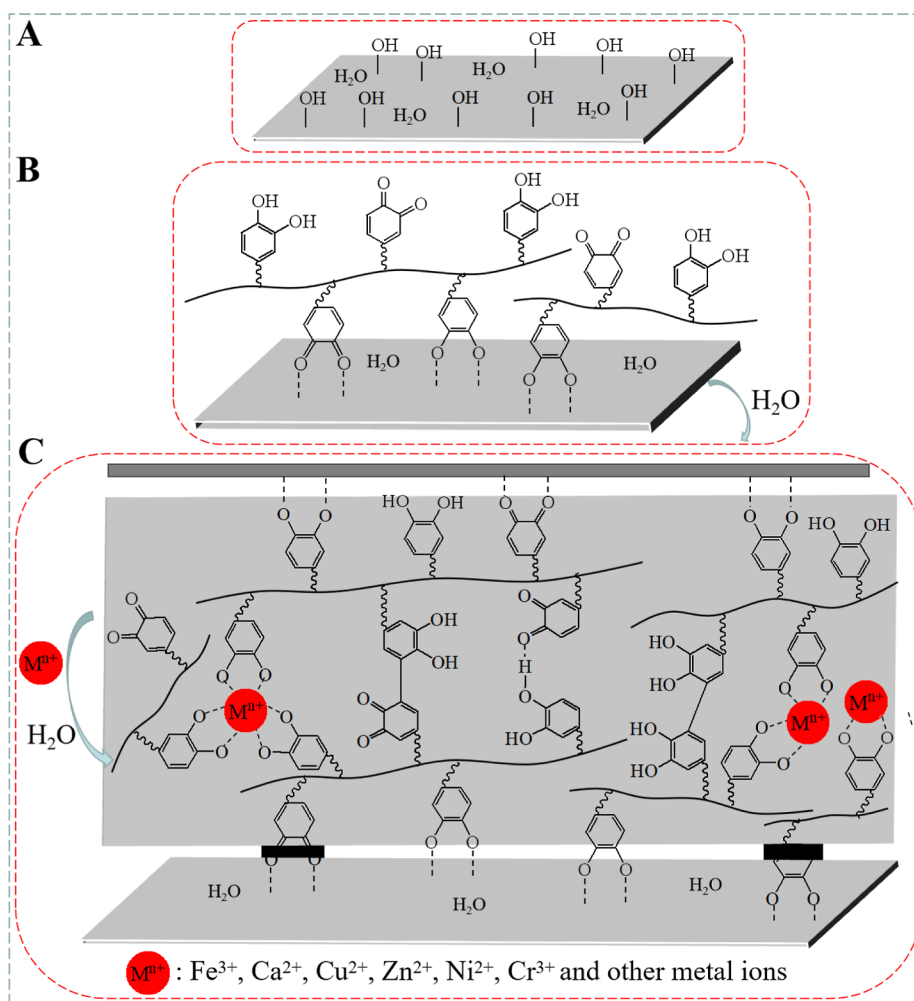


Figure 6. Plausible adhesion mechanisms of adhesives toward substrates: (A) active surface of substrates; (B) initial adhesion of cellulose-based adhesive to the wet surface of substrates: dashed lines present H-bonding, and the arrow demonstrates that water molecules are pushed back from the surface; and (C) the cross-sectional image of two substrates tied together in water; the arrow demonstrates that water molecules from the surroundings penetrate into the cellulose-based adhesive.

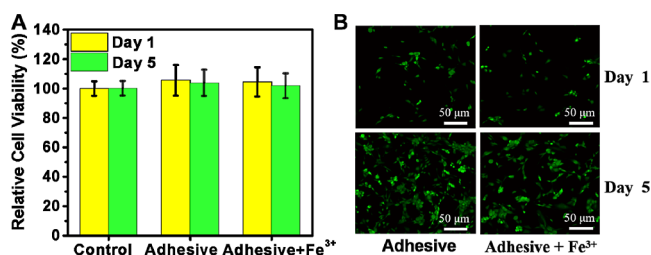


Figure 7. (A) Relative cell viability of the cellulose-based adhesive. (B) Images of cells cultured on adhesive.

triscatecholate complexes.²⁴ Compared to the adhesive with similar catechol content bonding to similar substrates (iron), the lap shear strength of the adhesive with Fe³⁺ is much stronger than that without Fe³⁺. The strongest lap shear strength of cellulose-based adhesives with a catechol content of 27.2 mol % is increased to 0.45 MPa on glass, 1.25 MPa on wood, 1.86 on aluminum, and 2.13 MPa on iron (Figure 4D). The lap shear strength is strongest on the iron substrate, followed by aluminum, wood, and glass. This is because glass material has lighter interfacial interactions with catechol elements and lesser surface roughness compared to other

substrates.^{44,45} Moreover, the lap shear strength of the cellulose-based adhesives on porcine skin was also measured. The strongest lap shear strength of cellulose-based adhesive with a catechol content of 27.2 mol % was 24.0 kPa (Supporting Information, Figure S2).

It is reported that the highest loads of polyethylene glycol diacrylate and dopamine copolymer on aluminum were ~1.2 MPa.¹³ Furthermore, the copolymer adhesive with 10% catechol and 90% styrene demonstrated an adhesive strength of 1.3 ± 0.2 MPa on aluminum.⁴⁶ These results suggest that the cellulose-based adhesives have strong lap shear strength in dry environments.

Figure 5A demonstrates the irons bound by the adhesive with a catechol content of 27.2 mol % underwater. The adherents could lift 500 g of weight and not be attracted apart underwater, representing that the cellulose-based adhesive has severe underwater adhesion.

The wet lap shear strength of cellulose-based adhesive with a catechol content of 27.2 mol % on iron is shown in Figure 5B. For the adhesive containing a catechol content of 4.6 mol %, the lap shear strengths of the adhesive were 0.05 MPa underwater and 0.09 MPa under seawater, respectively. With the increase of catechol content in adhesives, the lap shear

strength increases gradually. When the highest catechol content is 27.2 mol %, the lap shear strength of the adhesive increases to 0.10 and 0.16 MPa, respectively.

The highest adhesion strength of commercially available “Krazy Glue” was reported ≈ 5 kPa,⁴⁷ and epoxy, poly(vinyl acetate), and cyanoacrylate glues did not even permit the substrates to stay bonded when apprehended (ca. 0).⁴³ This shows that cellulose-based adhesive has strong underwater adhesion.

Catechol has strong underwater adhesion.^{1,19,48,49} As shown in Figure 6, the surface of the substrate has a partial hydroxyl group, which can be used as a hydrogen bond donor (Figure 6A), while the cellulose-based adhesives act as hydrogen bond acceptors, forming a strong hydrogen bond with the surface of the substrate (Figure 6B). This interaction is the interaction of catechol with the substrate surface, repelling water molecules from the surface and providing the initial adhesion of the copolymer to the wet surface. When the copolymer and metal ions are in contact with each other and plunged into water, the water molecules can gradually penetrate into the copolymer, promoting the diffusion of metal ions within the copolymer and allowing more uniform cross-linking and complexation of the two (Figure 6C). In addition, the metal ions in seawater will also penetrate into the bulk copolymer and coordinate with catechol groups to further increase the adhesive strength. They interact through catechol-Fe³⁺ chelation, oxidative cross-linking, π - π bonding, and coordination,^{50,51} allowing catechol-containing adhesive materials to adhere firmly to inorganic and organic substrates in a wet environment.

3.4. Biocompatibility. The biocompatibility of the adhesive was performed by NIH 3T3 cells, which is shown in Figure 7. After 1 day of cell culture, the relative cell viability of the cells on the adhesive was found to be 104 and 105% with and without Fe³⁺, respectively (Figure 7A). Meanwhile, after 5 days of cell culture, the relative cell viability of the cells is 101 and 103% with and without Fe³⁺, respectively. Previous literature demonstrated that a relative cell viability of less than 70% was regarded as cytotoxic.⁵² In addition, the cell morphology of the adhesive was studied. Results found that the cells developed on adhesives demonstrated a spread, irregular shape with protrusions after 1 and 5 days (Figure 7B), and the cell number increased significantly as the time prolonged. These results indicate that the prepared cellulose-based adhesives had excellent biocompatibility. Due to their good water resistance, our adhesive polymers cannot be dissolved into water. Therefore, it should be mentioned that organic solvents, such as DMSO, are needed for the dissolution of biocompatible adhesive polymers. Nevertheless, the adhesive polymers have a good biocompatibility and may be a promising candidate material for electronic devices.

4. CONCLUSIONS

In summary, we developed biocompatible cellulose-based underwater adhesives. The adhesives with a catechol content ranging from 4.6 to 27.2 mol % were prepared by grafting DOPMAM onto cellulose via the ATRP method. The lap shear strength increased with the increment of the catechol amount. Strong lap shear strength was realized on different substrates, with the highest adhesion strength of 1.47 MPa without Fe³⁺ and 2.13 MPa with Fe³⁺ in a dry environment. Meanwhile, the cellulose-based adhesive possessed underwater adhesion with 0.10 MPa underwater and 0.16 MPa under seawater. The adhesives exhibited excellent biocompatibility. The prepared

adhesives with excellent biocompatibility and underwater adhesion have potential applications in biomedicine, electronics, and construction fields.

■ ASSOCIATED CONTENT

Supporting Information

The Supporting Information is available free of charge at <https://pubs.acs.org/doi/10.1021/acsomega.3c07972>.

¹H NMR spectra of the protected DOPMAM and unprotected DOPMAM and lap shear strength of cellulose-based adhesives for porcine skin (PDF)

■ AUTHOR INFORMATION

Corresponding Authors

Xinxing Lin – School of Materials and Packaging Engineering, Fujian Polytechnic Normal University, Fuzhou, Fujian 350300, P. R. China; orcid.org/0009-0003-9018-1107; Phone: +86-18649784585; Email: fafuxin@163.com; Fax: +86-591-83715175

Ajoy Kanti Mondal – Institute of National Analytical Research and Service, Bangladesh Council of Scientific and Industrial Research, Dhanmondi, Dhaka 1205, Bangladesh; orcid.org/0000-0002-0982-0457; Email: ajoymondal325@yahoo.com

Hui Wu – College of Material Engineering, Fujian Agriculture and Forestry University, Fuzhou, Fujian 350108, P. R. China; National Forestry and Grassland Administration Key Laboratory of Plant Fiber Functional Materials, Fuzhou, Fujian 350108, P. R. China; orcid.org/0000-0002-9755-8371; Email: wuhuifafu@163.com

Authors

Zuwu Tang – School of Materials and Packaging Engineering, Fujian Polytechnic Normal University, Fuzhou, Fujian 350300, P. R. China; orcid.org/0009-0004-8334-1210

Meiqiong Yu – School of Materials and Packaging Engineering, Fujian Polytechnic Normal University, Fuzhou, Fujian 350300, P. R. China; College of Material Engineering, Fujian Agriculture and Forestry University, Fuzhou, Fujian 350108, P. R. China; National Forestry and Grassland Administration Key Laboratory of Plant Fiber Functional Materials, Fuzhou, Fujian 350108, P. R. China; orcid.org/0009-0008-5396-4897

Complete contact information is available at: <https://pubs.acs.org/10.1021/acsomega.3c07972>

Notes

The authors declare no competing financial interest.

■ ACKNOWLEDGMENTS

This work was supported by the Natural Science Foundation of Fujian Province (2023J05212 and 2021J05270) and the Education and Scientific Research Project for Young and Middle-aged Teachers of Fujian Province, China (JAT220249).

■ REFERENCES

- (1) Fan, H.; Gong, J. P. Bioinspired Underwater Adhesives. *Adv. Mater.* **2021**, *33* (44), 2102983.
- (2) Je, H.; Won, J. Natural urushiol as a novel under-water adhesive. *Chem. Eng. J.* **2021**, *404*, 126424.

- (3) Fu, Y.; Ren, P.; Wang, F.; Liang, M.; Hu, W.; Zhou, N.; Lu, Z.; Zhang, T. Mussel-inspired hybrid network hydrogel for continuous adhesion in water. *J. Mater. Chem. B* **2020**, *8* (10), 2148–2154.
- (4) Cholewinski, A.; Yang, F.; Zhao, B. Glycerol-Stabilized Algae-Mussel-Inspired Adhesives for Underwater Bonding. *Ind. Eng. Chem. Res.* **2020**, *59* (34), 15255–15263.
- (5) Cloete, W. E.; Focke, W. W. Fast underwater bonding to polycarbonate using photoinitiated cyanoacrylate. *Int. J. Adhes. Adhes.* **2010**, *30* (4), 208–213.
- (6) Zhou, J.; Wan, Y.; Liu, N.; Yin, H.; Li, B.; Sun, D.; Ran, Q. Epoxy adhesive with high underwater adhesion and stability based on low viscosity modified Mannich bases. *J. Appl. Polym. Sci.* **2018**, *135* (3), 45688.
- (7) Li, X.; Li, W.; Liu, Z.; Wang, X.; Guo, H.; Wang, R.; Guo, X.; Li, C.; Jia, X. Underwater polyurethane adhesive with enhanced cohesion by postcrosslinking of glycerol monomethacrylate. *J. Appl. Polym. Sci.* **2018**, *135* (32), 46579.
- (8) Lee, Y. J.; Jung, G. B.; Choi, S.; Lee, G.; Kim, J. H.; Son, H. S.; Bae, H.; Park, H.-K. Biocompatibility of a Novel Cyanoacrylate Based Tissue Adhesive: Cytotoxicity and Biochemical Property Evaluation. *PLoS One* **2013**, *8*, No. e79761.
- (9) Lee, D.; Hwang, H.; Kim, J.-S.; Park, J.; Youn, D.; Kim, D.; Hahn, J.; Seo, M.; Lee, H. VATA: A Poly(vinyl alcohol)- and Tannic Acid-Based Nontoxic Underwater Adhesive. *ACS Appl. Mater. Interfaces* **2020**, *12* (18), 20933–20941.
- (10) Waite, J. H.; Tanzer, M. L. Polyphenolic Substance of *Mytilus edulis*: Novel Adhesive Containing L-Dopa and Hydroxyproline. *Science* **1981**, *212* (4498), 1038–1040.
- (11) Waite, J. H. Adhesion a la Moule. *Integr. Comp. Biol.* **2002**, *42* (6), 1172–1180.
- (12) Wilker, J. J. Positive charges and underwater adhesion. *Science* **2015**, *349* (6248), 582–583.
- (13) Kaur, S.; Weerasekare, G. M.; Stewart, R. J. Multiphase Adhesive Coacervates Inspired by the Sandcastle Worm. *ACS Appl. Mater. Interfaces* **2011**, *3* (4), 941–944.
- (14) Wang, C. S.; Stewart, R. J. Multipart Copolyelectrolyte Adhesive of the Sandcastle Worm, *Phragmatopoma californica* (Fewkes): Catechol Oxidase Catalyzed Curing through Peptidyl-DOPA. *Biomacromolecules* **2013**, *14* (5), 1607–1617.
- (15) Zhao, Q.; Lee, D. W.; Ahn, B. K.; Seo, S.; Kaufman, Y.; Israelachvili, J. N.; Waite, J. H. Underwater contact adhesion and microarchitecture in polyelectrolyte complexes actuated by solvent exchange. *Nat. Mater.* **2016**, *15* (4), 407–412.
- (16) Fan, H.; Wang, J.; Tao, Z.; Huang, J.; Rao, P.; Kurokawa, T.; Gong, J. P. Adjacent cationic-aromatic sequences yield strong electrostatic adhesion of hydrogels in seawater. *Nat. Commun.* **2019**, *10*, 5127.
- (17) Fan, H.; Wang, J.; Gong, J. P. Barnacle Cement Proteins-Inspired Tough Hydrogels with Robust, Long-Lasting, and Repeatable Underwater Adhesion. *Adv. Funct. Mater.* **2021**, *31* (11), 2009334.
- (18) Ahn, B. K. Perspectives on Mussel-Inspired Wet Adhesion. *J. Am. Chem. Soc.* **2017**, *139* (30), 10166–10171.
- (19) Cui, C.; Liu, W. Recent Advances in Wet Adhesives: Adhesion Mechanism, Design Principle and Applications. *Prog. Polym. Sci.* **2021**, *116*, 101388.
- (20) Zhang, C.; Xiang, L.; Zhang, J.; Liu, C.; Wang, Z.; Zeng, H.; Xu, Z.-K. Revisiting the adhesion mechanism of mussel-inspired chemistry. *Chem. Sci.* **2022**, *13* (6), 1698–1705.
- (21) Xu, H.; Nishida, J.; Ma, W.; Wu, H.; Kobayashi, M.; Otsuka, H.; Takahara, A. Competition between Oxidation and Coordination in Cross-Linking of Polystyrene Copolymer Containing Catechol Groups. *ACS Macro Lett.* **2012**, *1* (4), 457–460.
- (22) Yu, M. E.; Hwang, J. Y.; Deming, T. J. Role of L-3,4-dihydroxyphenylalanine in mussel adhesive proteins. *J. Am. Chem. Soc.* **1999**, *121* (24), 5825–5826.
- (23) Liu, F.; Liu, X.; Chen, F.; Fu, Q. Mussel-Inspired Chemistry: A Promising Strategy for Natural Polysaccharides in Biomedical Applications. *Prog. Polym. Sci.* **2021**, *123*, 101472.
- (24) Tang, Z.; Zhao, M.; Wang, Y.; Zhang, W.; Zhang, M.; Xiao, H.; Huang, L.; Chen, L.; Ouyang, X.; Zeng, H.; Wu, H. Mussel-inspired cellulose-based adhesive with biocompatibility and strong mechanical strength via metal coordination. *Int. J. Biol. Macromol.* **2020**, *144* (1), 127–134.
- (25) Tang, Z.; Miao, Y.; Zhao, J.; Xiao, H.; Zhang, M.; Liu, K.; Zhang, X.; Huang, L.; Chen, L.; Wu, H. Mussel-inspired biocompatible polydopamine/carboxymethyl cellulose/polyacrylic acid adhesive hydrogels with UV-shielding capacity. *Cellulose* **2021**, *28* (3), 1527–1540.
- (26) Tang, Z.; Zhang, M.; Xiao, H.; Liu, K.; Li, X.; Du, B.; Huang, L.; Chen, L.; Wu, H. A Green Catechol-Containing Cellulose Nanofibrils-Cross-Linked Adhesive. *ACS Biomater. Sci. Eng.* **2022**, *8* (3), 1096–1102.
- (27) Tang, Z.; Yu, M.; Mondal, A. K.; Lin, X. Porous Scaffolds Based on Polydopamine/Chondroitin Sulfate/Polyvinyl Alcohol Composite Hydrogels. *Polymers* **2023**, *15* (2), 271.
- (28) Tang, Z.; Yu, M.; Yang, Y.; Pan, Y.; Mondal, A. K.; Lin, X. Development of an Antioxidant and UV-Shielding Composite Hydrogel Using Mussel-Inspired Cellulose Nanocrystals, Polydopamine, and Poly(vinyl alcohol) for Application in Sunscreens. *ACS Appl. Polym. Mater.* **2023**, *5* (8), 6625–6632.
- (29) Rol, F.; Belgacem, M. N.; Gandini, A.; Bras, J. Recent advances in surface-modified cellulose nanofibrils. *Prog. Polym. Sci.* **2019**, *88*, 241–264.
- (30) Rahmanian, V.; Pirzada, T.; Wang, S.; Khan, S. A. Cellulose-Based Hybrid Aerogels: Strategies toward Design and Functionality. *Adv. Mater.* **2021**, *33* (51), 2102892.
- (31) Lu, S.; Zhang, X.; Tang, Z.; Xiao, H.; Zhang, M.; Liu, K.; Chen, L.; Huang, L.; Ni, Y.; Wu, H. Mussel-inspired Blue-light-activated Cellulose-based Adhesive Hydrogel with Fast Gelation, Rapid Haemostasis and Antibacterial Property for Wound Healing. *Chem. Eng. J.* **2021**, *417*, 129329.
- (32) Jia, H.; Michinobu, T. Cellulose-based Conductive Gels and Their Applications. *ChemNanoMat* **2023**, *9* (5), No. e202300020.
- (33) Tang, Z.; Bian, S.; Wei, J.; Xiao, H.; Zhang, M.; Liu, K.; Huang, L.; Chen, L.; Ni, Y.; Wu, H. Plant-inspired conductive adhesive organohydrogel with extreme environmental tolerance as a wearable dressing for multifunctional sensors. *Colloids Surf., B* **2022**, *215*, 112509.
- (34) Liu, H.; Du, H.; Zheng, T.; Liu, K.; Ji, X.; Xu, T.; Zhang, X.; Si, C. Cellulose based composite foams and aerogels for advanced energy storage devices. *Chem. Eng. J.* **2021**, *426*, 130817.
- (35) Lv, P.; Lu, X.; Wang, L.; Feng, W. Nanocellulose-Based Functional Materials: From Chiral Photonics to Soft Actuator and Energy Storage. *Adv. Funct. Mater.* **2021**, *31* (45), 2104991.
- (36) Zhang, Z.; Wang, C.; Li, F.; Liang, L.; Huang, L.; Chen, L.; Ni, Y.; Gao, P.; Wu, H. Bifunctional Cellulose Interlayer Enabled Efficient Perovskite Solar Cells with Simultaneously Enhanced Efficiency and Stability. *Adv. Sci.* **2023**, *10* (8), 2207202.
- (37) Zhu, X.; Jiang, G.; Wang, G.; Zhu, Y.; Cheng, W.; Zeng, S.; Zhou, J.; Xu, G.; Zhao, D. Cellulose-based functional gels and applications in flexible supercapacitors. *Resour. Chem. Mater.* **2023**, *2* (2), 177–188.
- (38) Zhao, C.; Liu, G.; Tan, Q.; Gao, M.; Chen, G.; Huang, X.; Xu, X.; Li, L.; Wang, J.; Zhang, Y.; Xu, D. Polysaccharide-based biopolymer hydrogels for heavy metal detection and adsorption. *J. Adv. Res.* **2023**, *44*, 53–70.
- (39) Paul, J.; Ahankari, S. S. Nanocellulose-based aerogels for water purification: A review. *Carbohydr. Polym.* **2023**, *309*, 120677.
- (40) Tang, Z.; Lin, X.; Chen, Y.; Pan, Y.; Yang, Y.; Mondal, A. K.; Yu, M.; Wu, H. Preparation of mussel-inspired polydopamine-functionalized TEMPO-oxidized cellulose nanofiber-based composite aerogel as reusable adsorbent for water treatment. *Ind. Crop. Prod.* **2023**, *206*, 117735.
- (41) Tang, Z.; Bian, S.; Lin, Z.; Xiao, H.; Zhang, M.; Liu, K.; Li, X.; Du, B.; Huang, L.; Chen, L.; Ni, Y.; Wu, H. Biocompatible Catechol-Functionalized Cellulose-Based Adhesives with Strong Water Resistance. *Macromol. Mater. Eng.* **2021**, *306* (9), 2100232.

- (42) Ma, C.; Pang, H.; Cai, L.; Huang, Z.; Gao, Z.; Li, J.; Zhang, S. Facile strategy of mussel-inspired polymer as a high-performance dry/wet adhesive. *J. Clean. Prod.* **2021**, *308*, 127309.
- (43) White, J. D.; Wilker, J. J. Underwater Bonding with Charged Polymer Mimics of Marine Mussel Adhesive Proteins. *Macromolecules* **2011**, *44* (13), 5085–5088.
- (44) Li, A.; Jia, Y.; Sun, S.; Xu, Y.; Minsky, B. B.; Stuart, M. A. C.; Cölfen, H.; von Klitzing, R.; Guo, X. Mineral-Enhanced Polyacrylic Acid Hydrogel as an Oyster-Inspired Organic-Inorganic Hybrid Adhesive. *ACS Appl. Mater. Interfaces* **2018**, *10* (12), 10471–10479.
- (45) Liang, M.; He, C.; Dai, J.; Ren, P.; Fu, Y.; Wang, F.; Ge, X.; Zhang, T.; Lu, Z. A high-strength double network polydopamine nanocomposite hydrogel for adhesion under seawater. *J. Mater. Chem. B* **2020**, *8*, 8232–8241.
- (46) Matos-Perez, C. R.; Wilker, J. J. Ambivalent Adhesives: Combining Biomimetic Cross-Linking with Antiadhesive Oligo(ethylene glycol). *Macromolecules* **2012**, *45* (16), 6634–6639.
- (47) Li, A.; Jia, M.; Mu, Y.; Jiang, W.; Wan, X. Humid Bonding with a Water-Soluble Adhesive Inspired by Mussels and Sandcastle Worms. *Macromol. Chem. Phys.* **2015**, *216* (4), 450–459.
- (48) Li, A.; Mu, Y.; Jiang, W.; Wan, X. A mussel-inspired adhesive with stronger bonding strength under underwater conditions than under dry conditions. *Chem. Commun.* **2015**, *51* (44), 9117–9120.
- (49) Cai, C.; Chen, Z.; Chen, Y.; Li, H.; Yang, Z.; Liu, H. Mechanisms and applications of bioinspired underwater/wet adhesives. *J. Polym. Sci.* **2021**, *59* (23), 2911–2945.
- (50) Patil, N.; Jerome, C.; Detrembleur, C. Recent advances in the synthesis of catechol-derived (bio)polymers for applications in energy storage and environment. *Prog. Polym. Sci.* **2018**, *82*, 34–91.
- (51) Zhang, C.; Wu, B.; Zhou, Y.; Zhou, F.; Liu, W.; Wang, Z. Mussel-inspired hydrogels: from design principles to promising applications. *Chem. Soc. Rev.* **2020**, *49* (11), 3605–3637.
- (52) Liu, Y.; Meng, H.; Konst, S.; Sarmiento, R.; Rajachar, R.; Lee, B. P. Injectable Dopamine-Modified Poly(ethylene glycol) Nanocomposite Hydrogel with Enhanced Adhesive Property and Bioactivity. *ACS Appl. Mater. Interfaces* **2014**, *6* (19), 16982–16992.